

## Infrared study of the low-temperature-orthorhombic–low-temperature-tetragonal structural phase transition in $\text{La}_2\text{NiO}_4$

D. E. Rice

*Department of Chemical Engineering, University of Delaware, Newark, Delaware 19716*

M. K. Crawford

*Central Research and Development Department, E. I. du Pont de Nemours and Company, Experimental Station, P. O. Box 80356, Wilmington, Delaware 19880-0356*

D. J. Buttrey

*Department of Chemical Engineering, University of Delaware, Newark, Delaware 19716*

W. E. Farneth

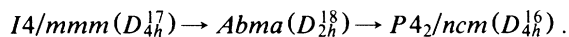
*Central Research and Development Department, E. I. du Pont de Nemours and Company, Experimental Station, P. O. Box 80356, Wilmington, Delaware 19880-0356*

(Received 2 July 1990)

We have studied the polarized infrared reflectance of a stoichiometric single crystal of  $\text{La}_2\text{NiO}_4$  through the  $Abma (D_{2h}^{17})$  (low-temperature orthorhombic)  $\rightarrow P4_2/nm (D_{4h}^{16})$  (low-temperature tetragonal) structural phase transition. This transition, which occurs near 70 K, involves a rigid tilt of the  $\text{Ni-O}_6$  octahedra and produces distinct changes in the infrared-active phonons. Our observations are consistent with a first-order phase transition. This phase transition also occurs in  $\text{La}_{1.88}\text{Ba}_{0.12}\text{CuO}_4$ , and has a profound influence on superconductivity in that material.

### INTRODUCTION

The layered material  $\text{La}_2\text{NiO}_{4+\delta}$  has been the subject of numerous investigations because of its unusual structural and magnetic properties.<sup>1–3</sup> The availability of large, high-quality single crystals<sup>4</sup> of  $\text{La}_2\text{NiO}_{4+\delta}$  also provides unique opportunities for detailed study of relationships to the isostructural  $\text{La}_{2-x}\text{M}_x\text{CuO}_4$  ( $M = \text{Sr}, \text{Ba}$ ) family.<sup>5</sup> Recently, an additional important correspondence has emerged between  $\text{La}_2\text{NiO}_4$  and  $\text{La}_{2-x}\text{Ba}_x\text{CuO}_4$ . The latter material, for  $x \approx 0.12$ , has been observed<sup>6</sup> to undergo the following sequence of structural phase transitions between 300 and 10 K:<sup>7</sup>



The  $Abma$  (LTO, low-temperature orthorhombic) and  $P4_2/nm$  (LTT, low-temperature tetragonal) structures are shown in Fig. 1. These phase transitions involve successive rigid Cu-O octahedra tilts of equal magnitude about the  $[110]$  and  $[\bar{1}\bar{1}0]$  axes of the  $I4/mmm$  phase. The first transition is continuous (second order), whereas the second transition is apparently discontinuous<sup>6</sup> (first order). The  $Abma \rightarrow P4_2/nm$  lattice instability influences the transition to the superconducting state<sup>8</sup> in doped  $\text{La}_2\text{CuO}_4$ . In fact, the  $P4_2/nm$  phase appears not to superconduct.  $\text{La}_2\text{NiO}_4$  undergoes the same sequence of structural transitions when the composition is close to the ideal oxygen stoichiometry,<sup>2</sup> i.e.,  $\text{La}_2\text{NiO}_{4.000 \pm 0.005}$ . Therefore, it is possible to study these structural transitions in the absence of free carriers using single crystals of  $\text{La}_2\text{NiO}_{4+\delta}$ .

Here we report a detailed infrared spectroscopic study of the LTO  $\rightarrow$  LTT structural phase transition in

stoichiometric single crystals of  $\text{La}_2\text{NiO}_4$ . Unlike a previous infrared study<sup>9</sup> of  $\text{La}_2\text{NiO}_{4+\delta}$ , where the significant oxygen nonstoichiometry produced an  $ab$ -plane free-carrier plasma which screened the in-plane phonon response, our stoichiometric crystals allow clear observation of all infrared-active phonons. We clearly observe the phase transition using infrared polarizations either along the  $c$  axis or in the  $ab$  plane. The LTO  $\rightarrow$  LTT phase transition is expected to be first order on the basis of symmetry considerations.<sup>10</sup> The infrared data are consistent with this expectation.

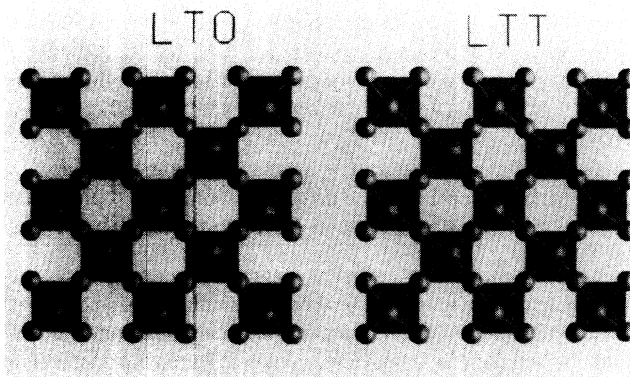


FIG. 1. The LTO and LTT tilt structures of  $\text{La}_2\text{NiO}_4$ . The tilt angles are slightly exaggerated for clarity. The adjacent Ni-O sheets for the LTT structure are rotated by  $90^\circ$  about the axis perpendicular to the sheet, producing tetragonal symmetry. Note that if the successive orthogonal octahedra tilts which yield the LTT structure were of different magnitude, the  $Pccn$  structure would be obtained.

## EXPERIMENT

Single crystals of  $\text{La}_2\text{NiO}_{4+\delta}$  were grown by a radio-frequency skull-melting technique.<sup>4</sup> Samples were oriented by Laue diffraction and subsequently cut and polished to yield faces parallel and perpendicular to the  $c$  axis. The oxygen stoichiometry was then fixed by a controlled anneal at 1273 K in a  $\text{CO-CO}_2$  flowing-gas atmosphere in which the oxygen fugacity was measured with a  $\text{Y}_2\text{O}_3$ -stabilized  $\text{ZrO}_2$  cell at ( $\log_{10}f_{\text{O}_2} = -11.1$ ), closely approaching the reduction boundary at which the stoichiometric limit is expected.<sup>11</sup> Thin sections ( $< 200 \mu\text{m}$  thick) of crystals prepared in this manner are amber colored.

The infrared methods have been described previously.<sup>12</sup> Various wire-grid polarizers were utilized to separate the  $c$ -axis and  $ab$ -plane reflectance. The spectra were fit with an oscillator model in which the frequency-dependent dielectric constant was calculated as the product of individual oscillators. Similar mode frequencies and oscillator strengths were obtained either by fitting the data to a sum-of-oscillators model, or performing Kramers-Kronig analysis of the reflectance data.

## RESULTS AND DISCUSSION

Between  $\sim 700$  and 70 K, stoichiometric  $\text{La}_2\text{NiO}_4$  is orthorhombic,<sup>1,2</sup> space group  $Abma(D_{2h}^{18})$ . In the  $Abma$  (and  $Bmab$ ) space group the  $c$  axis is the long axis, consistent with the situation in both  $I4/mmm$  and  $P4_2/nmc$  symmetry. A group-theoretical analysis of the Brillouin-zone-center vibrations for the  $Abma$  structure leads to the following mode assignments grouped according to their activity;<sup>10</sup> infrared ( $6B_{1u} + 4B_{2u} + 7B_{3u}$ ), Raman ( $5A_g + 4B_{1g} + 6B_{2g} + 4B_{3g}$ ), acoustic ( $B_{1u} + B_{2u} + B_{3u}$ ), silent ( $4A_u$ ). There are 17 ir-active phonons. Since the crystals are twinned we cannot separate the  $B_{2u}$  ( $a$  axis) from the  $B_{3u}$  ( $b$  axis) modes. We thus measure all  $4B_{2u} + 7B_{3u}$  modes with  $ab$ -plane polarization. The  $c$ -axis-polarized modes ( $6B_{1u}$ ), however, can be easily separated from the  $ab$ -plane modes.

The group-theoretical results for the tetragonal  $P4_2/nmc(D_{4h}^{16})$  structure give mode activities as follows: infrared ( $7A_{2u} + 12E_u$ ), Raman ( $5A_{1g} + 3B_{1g} + 5B_{2g} + 10E_g$ ), acoustic ( $A_{2u} + E_u$ ), silent ( $3A_{1u} + 8B_{1u} + 3B_{2u} + 3A_{2g}$ ). The infrared active modes separate into  $7A_{2u}$  ( $c$  axis polarized) and  $12E_u$  ( $ab$  plane polarized) phonons. We note that the primitive cell for this structure has twice

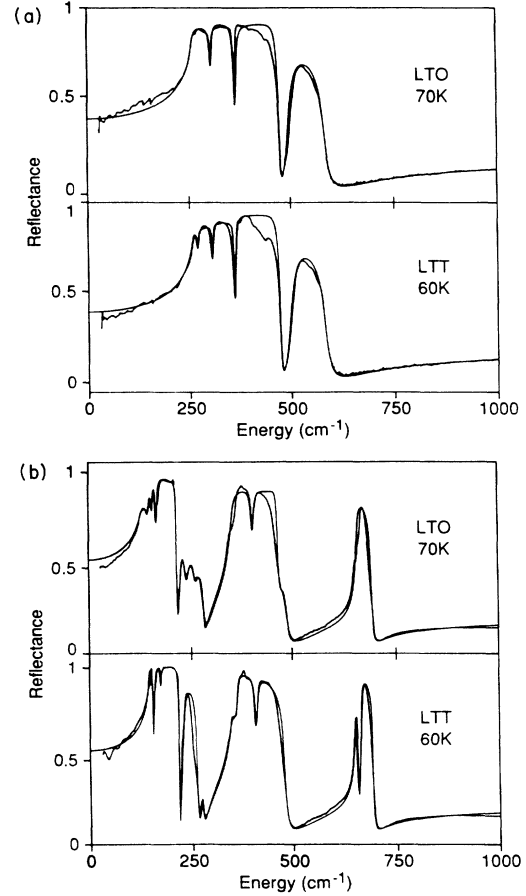


FIG. 2. (a) Infrared reflectance of  $\text{La}_2\text{NiO}_4$  at 70 K (LTO structure) and 60 K (LTT structure). The infrared polarization is along the  $c$  axis. Note the new mode at  $274 \text{ cm}^{-1}$  in the LTT phase. (b) Infrared reflectance of  $\text{La}_2\text{NiO}_4$  at 70 K (LTO structure) and 60 K (LTT structure). The infrared polarization is in the  $ab$  plane. There are clear changes in the infrared-active phonons due to the phase transition. In (a) and (b), oscillator fits are superimposed on the data (see Tables I and II).

the volume of the  $Abma$  primitive cell. Consequently, the  $\text{LTO} \rightarrow \text{LTT}$  phase transition folds the  $Z$ -point phonons in the  $Abma$  Brillouin zone over to the  $P4_2/nmc$  zone center.<sup>6</sup> Thus the total number of ir-active modes is larger for the LTT structure than for the LTO structure despite the increased symmetry of the low-temperature phase.

In Fig. 2(a) we show the  $c$ -axis-polarized reflectance

TABLE I. Oscillator fit parameters for the  $c$ -axis-polarized phonons in the LTO and LTT phases of  $\text{La}_2\text{NiO}_4$ . Transverse-optic mode ( $\omega_{\text{TO}}$ ) and longitudinal-optic mode ( $\omega_{\text{LO}}$ ) energies in  $\text{cm}^{-1}$ , damping ( $\gamma = \gamma_{\text{TO}} = \gamma_{\text{LO}}$ ) in  $\text{cm}^{-1}$ , and oscillator strength  $S$ , determined by solving  $\epsilon(\omega) = \epsilon_{\infty} [1 + \sum_i S_i \omega_{\text{TO},i}^2 / (\omega_{\text{TO},i}^2 - \omega^2 - i\gamma\omega)]$ , with  $\gamma$  set to zero and  $\omega$  set to  $\omega_{\text{LO}}$  [i.e.,  $\epsilon(\omega_{\text{LO}}) = 0$ ].  $\epsilon_{\infty} = 0.5$  for the LTO and LTT phases.

LTO [ $Bmab(D_{2h}^{18})$ ], $B_{1u}$ modes, $T=70$ K				LTT [ $P4_2/nmc(D_{4h}^{16})$ ], $A_{2u}$ modes, $T=60$ K			
$\omega_{\text{TO}}$	$\omega_{\text{LO}}$	$\gamma$	$S$	$\omega_{\text{TO}}$	$\omega_{\text{LO}}$	$\gamma$	$S$
261	306.5	7	3.173	259.5	269.5	8	2.046
309.5	365	6	0.137	274.3	306.2	8.5	0.835
369.5	475.5	6.5	0.062	310	361	7.5	0.177
496	585	16	0.046	366.5	475	5.5	0.081
				500	585	16	0.052

TABLE II. Oscillator fit parameters for the  $ab$ -plane-polarized phonons in the LTO and LTT phases of  $\text{La}_2\text{NiO}_4$ . Symbols are defined in the heading for Table I.  $\epsilon_\infty=4.8$  for the LTO and LTT phases.

LTO [ $Bmab(D_{2h}^2)$ ], $B_{2u}$ and $B_{3u}$ modes, <sup>a</sup> $T=70$ K				LTT [ $P4_2/ncm(D_{2h}^2)$ ], $E_u$ modes, $T=60$ K			
$\omega_{\text{TO}}$	$\omega_{\text{LO}}$	$\gamma$	$S$	$\omega_{\text{TO}}$	$\omega_{\text{LO}}$	$\gamma$	$S$
131	146.5	13.5	4.357	142	152.8	2	3.284
149	154.3	5.5	0.365	157.4	171.2	2.4	1.062
156.8	165.8	4.3	0.387	171.7	217	2.7	0.063
168.5	216.5	3.8	0.314	228	263	6.5	0.166
226	237.5	12.5	0.109	273	277	7	0.013
244.5	261	18	0.091	348	359.5	15	0.425
267	282.5	16.7	0.039	362.5	408.2	8	0.101
353	403.7	8	0.493	410.4	480	8	0.012
405.6	468	8	0.012	652.7	661	4	0.046
470	486.5	16.5	0.001	667	696	2.7	0.023
660	696	4.7	0.063				

<sup>a</sup>Due to crystal twinning, we observe the total of  $4B_{2u} + 7B_{3u}$  modes.

spectrum for a single crystal of  $\text{La}_2\text{NiO}_4$  at 70 and 60 K. Oscillator fits to the reflectance data are superimposed on the raw spectra, and fitted parameters are listed in Table I. In the 70-K spectrum we observe four of the six  $B_{1u}$  modes predicted by group theory for the LTO structure. In the 60-K spectrum, we observe five of the  $7A_{2u}$  phonons predicted for the LTT structure. Thus one additional  $c$ -axis-polarized phonon appears below the phase transition, as expected. The two unobserved modes in each phase most likely have small oscillator strengths, high damping, or energies of less than  $30\text{ cm}^{-1}$ . There are weak features in the reflectance data, in particular near  $400\text{ cm}^{-1}$ , that exhibit some temperature dependence, and which may be associated with these additional modes. We have not attempted to fit these features. In Fig. 2(b) we show similar data at 70 and 60 K for  $ab$  polarization. The results of the oscillator fit are given in Table II. In the LTO phase we observe all eleven phonons expected from group theory ( $4B_{2u} + 7B_{3u}$ ). In the LTT phase we

observe ten of the predicted  $12E_u$  phonons. There are clear changes in the  $ab$ -plane modes as a result of the phase transition. For example, the TO phonon at  $660\text{ cm}^{-1}$  in the LTO phase is replaced by two TO modes, one at  $653\text{ cm}^{-1}$  and the other at  $667\text{ cm}^{-1}$  in the LTT phase.

In Figs. 3 and 4,  $c$ -axis-polarized and  $ab$ -plane-polarized spectra for various temperatures between 60 and 70 K, the temperature range over which the phase transition occurs, are shown. Evidence in both polarizations suggests that this is a first-order (discontinuous) phase transition. For example, in Fig. 2(b), the oscillator strength for the TO phonon at  $274\text{ cm}^{-1}$  associated with the LTT phase remains essentially constant over the  $10^\circ$  temperature range. This is indicated by the constant TO-LO splitting of this mode at all temperatures (determined from oscillator fits). This behavior is inconsistent with a second-order (continuous) phase transition. Similarly, in  $ab$  polarization, the TO mode at  $653\text{ cm}^{-1}$  has a

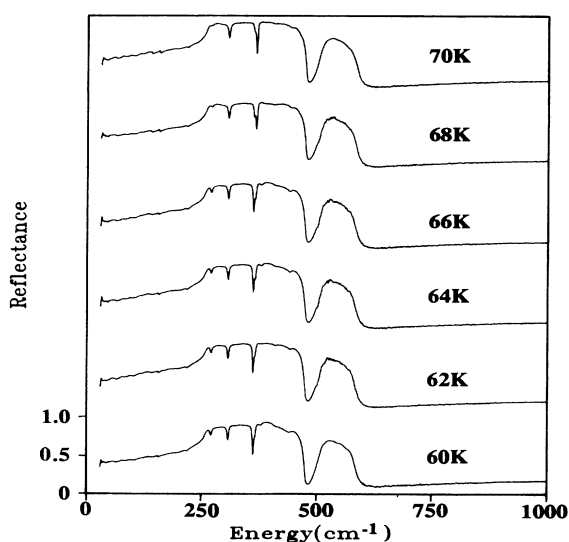


FIG. 3. Infrared reflectance at six temperatures for  $\text{La}_2\text{NiO}_4$ . The infrared polarization is parallel to the  $c$  axis.

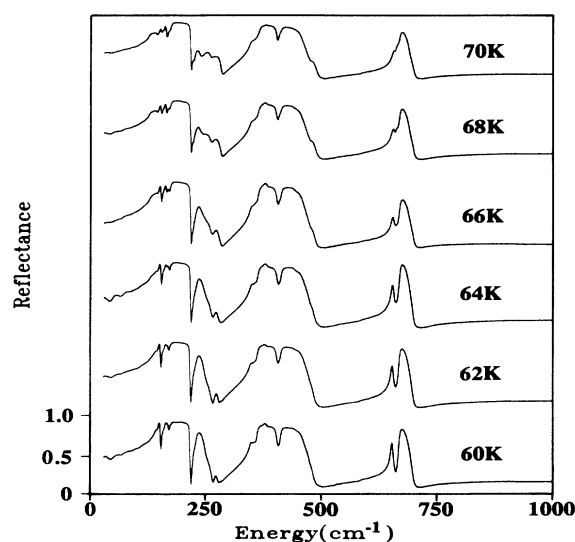


FIG. 4. Infrared reflectance at six temperatures for  $\text{La}_2\text{NiO}_4$ . The infrared polarization is in the  $ab$  plane.

temperature-independent TO-LO splitting. We therefore believe that the apparent 10-K width of the phase transition originates from phase coexistence (i.e., LTO and LTT) due to oxygen inhomogeneity. In fact, we can fit the reflectance data for  $60\text{ K} < T < 70\text{ K}$  quite well by assuming that all spectra are weighted sums of the 60- and 70-K spectra, corresponding to temperature-dependent fractions of the LTO and LTT phases. These observations are consistent with a first-order LTO  $\rightarrow$  LTT phase transition.<sup>10</sup> Neutron-diffraction data also indicate a discontinuous transition.<sup>2</sup> It is of interest that previous ultrasound measurements<sup>13</sup> of the LTT  $\rightarrow$  LTO transition in isostructural  $(\text{CH}_3\text{NH}_3)_2\text{MnCl}_4$  indicated a large softening of the  $c_{66}$  shear mode in the LTT phase as the temperature was increased. This was interpreted as evidence for an intermediate *Pccn* structure which, although unstable to either the LTT or LTO structures at any temperature, could impart a strong second-order character to the LTO  $\rightarrow$  LTT phase transition. We see no evidence for this in the infrared data.

The phonons that we observe may be grouped into two sets. The high-frequency modes ( $500\text{--}700\text{ cm}^{-1}$ ) involve mostly motion of apical oxygen atoms ( $B_{1u}$ - or  $A_{2u}$ -symmetry phonons in the LTO or LTT phase, respectively) or in-plane oxygen atoms ( $B_{2u}$ ,  $B_{3u}$ , or  $E_u$  symmetries in the LTO or LTT phase, respectively). The lower-frequency phonons ( $200\text{--}500\text{ cm}^{-1}$ ) are Ni-O bond-

bending vibrations and translational vibrations of the La atoms. A complete symmetry analysis for the LTO  $\rightarrow$  LTT phase transition in  $(\text{CH}_3\text{NH}_3)_2\text{MnCl}_4$ , is given in Ref. 10. In particular, this reference includes symmetry-adapted vectors for the LTO  $Z$ -point phonons which fold over to  $\Gamma$ -point modes in the LTT phase. It also lists correlations between the irreducible representations of the phonons in the various space groups adopted by  $\text{La}_2\text{NiO}_4$ .

In conclusion, we have reported polarized infrared reflectance observations of the *Abma*  $\rightarrow$  *P4<sub>2</sub>/ncm* structural phase transition in stoichiometric single crystals of  $\text{La}_2\text{NiO}_4$ . We observe clear changes in the infrared-active phonons due to the phase transition, and these changes are consistent with a discontinuous (first order) structural transformation. Thus  $\text{La}_2\text{NiO}_4$  serves as an excellent lattice dynamical prototype for the LTO  $\rightarrow$  LTT phase transition in  $\text{La}_{1.88}\text{Ba}_{0.12}\text{CuO}_4$  without additional complications due to the presence of charge carriers.

#### ACKNOWLEDGMENTS

The authors thank R. J. Smalley for technical assistance. The authors are also grateful to R. French and G. Burns for help with the oscillator fitting routines and to J. Calabrese for Fig. 1. Work at the University of Delaware was supported by the NSF under Contract No. DMR-8914080.

<sup>1</sup>G. Aeppli and D. J. Buttrey, *Phys. Rev. Lett.* **61**, 203 (1988); T. Freltoft, D. J. Buttrey, G. Aeppli, D. Vaknin, and G. Shirane, *Phys. Rev. B* (to be published).

<sup>2</sup>G. H. Lander, P. J. Brown, J. Spalek, and J. M. Honig, *Phys. Rev. B* **40**, 4463 (1989).

<sup>3</sup>J. D. Jorgensen, B. Dabrowski, S. Pei, D. R. Richards, and D. G. Hinks, *Phys. Rev. B* **40**, 2187 (1989).

<sup>4</sup>D. J. Buttrey, H. R. Harrison, J. M. Honig, and R. R. Schartman, *J. Solid State Chem.* **54**, 407 (1984).

<sup>5</sup>G. Aeppli *et al.*, *Physica C* **153-155**, 1111 (1988).

<sup>6</sup>J. D. Axe, A. H. Moudden, D. Hohlwein, D. E. Cox, K. M. Mohanty, A. R. Moodenbaugh, and Youwen Xu, *Phys. Rev. Lett.* **62**, 2751 (1989).

<sup>7</sup>G. Burns and A. M. Glazer, *Space Groups for Solid State Scientists* (Academic, New York, 1989). We have chosen to use the *Abma*( $D_{2h}^8$ ) designation for the space group of the low-temperature orthorhombic phase in order to be consistent

with previous work on the spectroscopy of this and related systems. This space group is equivalent to the *Bmab* and *Cmca* space groups under appropriate coordinate transformations.

<sup>8</sup>M. K. Crawford, M. L. Kunchur, W. E. Farneth, E. M. McCarron III, and S. J. Poon, *Phys. Rev. B* **41**, 282 (1990); M. K. Crawford, W. E. Farneth, E. M. McCarron III, R. L. Harlow, and A. H. Moudden, *Science* (to be published).

<sup>9</sup>J.-M. Bassat, P. Odier, and F. Gervais, *Phys. Rev. B* **35**, 7126 (1987).

<sup>10</sup>R. Geick and K. Strobel, *J. Phys. C* **10**, 4221 (1977).

<sup>11</sup>R. R. Schartman and J. M. Honig, *Mater. Res. Bull.* **24**, 375 (1989).

<sup>12</sup>M. K. Crawford, W. E. Farneth, E. M. McCarron III, and R. K. Bordia, *Phys. Rev. B* **38**, 11382 (1988).

<sup>13</sup>T. Goto, B. Luthi, R. Geick, and K. Strobel, *Phys. Rev. B* **22**, 3452 (1980).

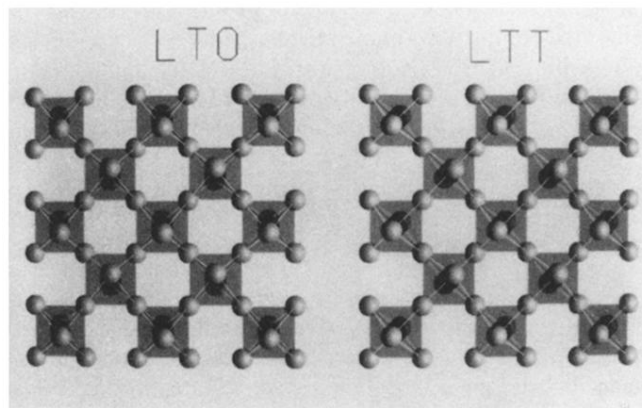


FIG. 1. The LTO and LTT tilt structures of  $\text{La}_2\text{NiO}_4$ . The tilt angles are slightly exaggerated for clarity. The adjacent Ni-O sheets for the LTT structure are rotated by  $90^\circ$  about the axis perpendicular to the sheet, producing tetragonal symmetry. Note that if the successive orthogonal octahedra tilts which yield the LTT structure were of different magnitude, the  $Pccn$  structure would be obtained.